

Tight and Compact Sample Average Approximation for Joint Chance Constrained Optimal Power Flow

Álvaro Porras^a, Concepción Domínguez^a, Juan Miguel Morales^{a,*}, Salvador Pineda^a

^a*Optimization and Analytics for Sustainable energy Systems (OASYS), University of Málaga, 29071 Málaga (Spain)*

Abstract

We tackle the resolution of a probabilistically-constrained version of the DC Optimal Power Flow problem with uncertain demand. The chance constraint requires that the probability of violating *any* of the power system's constraints be lower than some parameter $\epsilon > 0$. We use Sample Average Approximation to produce a data-driven deterministic reformulation of the problem, which takes the form of a large-scale mixed-integer program cursed with Big-Ms. We then introduce an exact resolution method for the MIP that combines the addition of a set of valid inequalities to tighten the linear relaxation bound with coefficient strengthening and constraint screening algorithms to improve its Big-Ms and considerably reduce its size. The proposed valid inequalities are based on the notion of *k-envelopes*, can be computed offline using polynomial-time algorithms, and added to the MIP program all at once. Furthermore, they are equally useful to boost the strengthening of the Big-Ms and the screening rate of superfluous constraints. In a series of numerical experiments which involve five power systems of different size, we show the efficiency of the proposed methodology and compare it with some of the best-performing convex inner approximations currently available in the literature.

Keywords: Chance Constraints, Probabilistic Constraints, *k*-Violation Problems, Combinatorial Optimization, Mixed Integer Programming, Valid Inequalities, Optimal Power Flow

1. Introduction

The Optimal Power Flow (OPF) problem is a routine at the core of important tools for power system operations (Frank et al. (2012)). The OPF problem seeks to determine the production levels of generating units that satisfy the power (net) demand at minimum cost while complying with some technical constraints imposed by those units and the grid. The main challenge of the OPF is that it is a non-linear and non-convex optimization problem, due to the power flow equations that govern the (static) behavior of power systems. For this reason, the *direct current* approximation (DC) of the power flow equations, which transforms the problem into a linear program, is frequently used. The demand and renewable generation are factors that increase the uncertainty in power systems, and ignoring it can lead to unsafe operating conditions.

Chance-constrained programming suits applications in areas where decisions have to be made dealing with random parameters (Miller & Wagner (1965)). In these situations, it is desirable to ensure feasibility of the system almost surely, but there is hardly any decision which would guarantee it under extreme events or unexpected random

*Corresponding author

Email address: juan.morales@uma.es (Juan Miguel Morales)

circumstances. In the context of the OPF, chance-constrained programming can be used to minimize the expected operating cost whilst guaranteeing that the system withstands unforeseen peaks of electrical load due to stochastic demand or uncertainty in power generation (Van Ackooij et al. (2011)). The chance-constrained OPF (CC-OPF) problem addresses this uncertainty and pursues to ensure the safe operation of a power system with a high level of probability. Under a linear approximation of the power flow equations, the CC-OPF problem can be formulated as the following chance-constrained problem (CCP) with joint linear chance constraints and random RHS and LHS:

$$\min_x f(x) \tag{1a}$$

$$\text{s.t. } x \in X \tag{1b}$$

$$\mathbb{P} \{a_j(\omega)^\top x \leq b_j(\omega), \forall j \in \mathcal{J}\} \geq 1 - \epsilon. \tag{1c}$$

In (1), $x \in \mathbb{R}^{|\mathcal{I}|}$ is a vector of continuous decision variables, $X \subseteq \mathbb{R}^{|\mathcal{I}|}$ is a polyhedron that represents a set of deterministic constraints, and $f : \mathbb{R}^{|\mathcal{I}|} \rightarrow \mathbb{R}$ is a convex function. Uncertainty is represented through the random vector ω taking values in \mathbb{R}^d and giving rise to a technology matrix with random rows $a_j(\omega) \in \mathbb{R}^{|\mathcal{I}|}$, $j \in \mathcal{J}$ and random $b_j(\omega) \in \mathbb{R}$, $j \in \mathcal{J}$. \mathbb{P} is a probability measure, and ϵ is a confidence or risk parameter, typically near zero, so that the set of constraints (1c) are satisfied with probability at least $(1 - \epsilon)$. Apart from power systems, applications of CCPs include supply chain, location and logistics (Taleizadeh et al. (2012), Shaw et al. (2016), Elçi et al. (2018)), risk control in finance (Daniélsson et al. (2008), Natarajan et al. (2008)), and healthcare problems such as operating room planning (Najjarbashi & Lim (2020)) or vaccine allocation (Tanner et al. (2008)), among others.

When the probabilistic constraint corresponds to (1c), the CCP has joint chance constraints (JCC) and is hence classified as a joint CCP (JCCP), in contrast with single CCPs (SCCPs), i.e. CCPs with individual or single chance constraints (SCC) of the form $\mathbb{P} \{a_j(\omega)^\top x - b_j(\omega) \leq 0\} \geq 1 - \epsilon_j, \forall j \in \mathcal{J}$. JCCPs are suitable for contexts where all constraints need to be simultaneously satisfied with a high probability, and the dependence between random variables makes them clearly harder. Both SCCPs and JCCPs have been extensively studied (see Prékopa (2003), Van Ackooij et al. (2011) and the references therein).

There are a number of reasons why general CCPs are challenging. The first one is the non-convexity of the feasible set. In general, the feasible region of a CCP is not convex in the original space even when x is continuous, there is only RHS uncertainty and the constraints inside the probability in (1c) result in a polyhedral region (Küçükyavuz & Jiang (2021)). To circumvent this problem, several approaches have been proposed. Some methods (e.g. Lagoa et al. (2005), Henrion (2007), Henrion & Strugarek (2011)) give convexity results and investigate the conditions under which the feasible region of problem (1) is convex. In another line of research, various convex approximation schemes such as quadratic (Ben-Tal & Nemirovski (2000)) or Bernstein approximation (Nemirovski & Shapiro (2007)), have been proposed in the literature. The CVaR approximation has gained a lot of popularity since its introduction (Rockafellar & Uryasev (2000), Sun et al. (2014)), and remains one of the most used methods to deal with stochastic problems. Nonetheless, the solutions to the approximated problems err on the side of over-conservatism. In this context, some iterative schemes such as ALSO-X have been recently proposed to identify tighter inner convex approximations of the CCP at the expense of a higher computational cost (Ahmed et al. (2017), Jiang & Xie (2022)). Finally, other works suggest convex approximations for non-linear CCPs. For instance, Hong et al. (2011) propose to solve the JCCP by a sequence of convex approximations followed by a gradient-based Monte

Carlo method, whereas Peña-Ordieres et al. (2020) introduce a smooth sampling-based approximation.

The second difficulty of CCPs is that checking the feasibility of a given solution is not, in general, an easy task. For instance, even if the uncertainty follows a known continuous distribution, calculating the joint probability requires a multi-dimensional integration, which becomes increasingly difficult with the dimension of the random vector ω . On top of that, in most cases the distribution \mathbb{P} is not fully known. To cope with these two obstacles at once, in this work we make use of Sample Average Approximation (SAA), which in practice boils down to dealing with a finite discrete distribution. The application of SAA may be seen as the result of approximating a general known distribution via the generation of independent Monte Carlo samples of the random vector ω (Shapiro (2003), Nemirovski & Shapiro (2006)) or as a data-driven approach that works with observations of ω that are available to the decision-maker even if the distribution is unknown.

SAA allows for a deterministic reformulation of the problem, and the resulting model is a mixed-integer problem (MIP). For the resolution of CCPs using MIP reformulations, we refer the reader to Küçükyavuz & Jiang (2021). When there is only RHS uncertainty (i.e. the technology matrix is fixed), a reformulation of the problem leads to a MIP with a set of constraints that form a *mixing set* and that have been extensively studied, alone or in combination with the knapsack constraint that also appears in the formulation (Günlük & Pochet (2001), Luedtke et al. (2010), Abdi & Fukasawa (2016)). Alternative reformulations like the ones proposed by Dentcheva et al. (2000), Nair & Miller-Hooks (2011) rely on the concept of $(1 - \epsilon)$ -efficient points. The case when the technology matrix is random, while the RHS is not, has been studied e.g. in Tayur et al. (1995). As for the general case, it has also been addressed in the literature. Specifically, a large line of research has focused on the development of *quantile cuts*, a particular type of valid inequality that can be viewed as a projection of a set of mixing inequalities for the MIP onto the original problem space. These cuts and the associated quantile closure have been recently studied in Qiu et al. (2014), Xie & Ahmed (2016, 2018), Ahmed & Xie (2018) and successfully applied to computational experiments of CCPs in Song et al. (2014), Ahmed et al. (2017), among others.

To address the CC-OPF problem, several papers in the literature (e.g., Roald & Andersson (2018)) directly work with SCCs. However, the main drawback of this modeling approach is that, even in those cases where the probability of violating each individual constraint seems more than tolerable, the resulting *joint risk* (that is, the probability that *any* of the technical constraints be violated) may still be excessive and inadmissible. This is the key motivation behind the use of JCCs to tackle the CC-OPF problem (see, e.g., Peña-Ordieres et al. (2021)). It is also true that there are ways to guarantee the satisfaction of the joint chance-constraint system by way of SCCs. Unfortunately, the success of this strategy depends on the non-trivial task of how to allocate the joint risk of the system among the single constraints. For example, based on Bonferroni's inequality, distributing the joint risk evenly across all individual constraints ensures that the joint chance constraint is met. However, this results in a rather conservative solution in general. To reduce the conservatism of this solution approach, Baker & Bernstein (2019) propose a learning algorithm to filter out redundant constraints and, thus, increase the risk of the non-redundant ones, whereas Jia et al. (2021) devise a non-parametric iterative framework to allocate the joint risk. In contrast to these works, we explicitly model and deal with the joint chance constrained version of the problem.

In this vein, there are several approaches in the literature to solve the JCC-OPF problem. Vrakopoulou et al. (2013) adopt the scenario approach (SA) to approximate the solution of the JCC-OPF, while Chen et al. (2021)

propose a heuristic data-driven method that involves enforcing the satisfaction of the technical constraints for a box of the uncertainty. This box is inferred using one-class support vector clustering and its size is contingent on the system’s desired reliability. Hou & Roald (2020) propose an iterative tuning algorithm to solve a robust reformulation of the JCC-OPF problem. Esteban-Pérez & Morales (2021) introduce a distributionally robust JCC-OPF model that considers contextual information using an ambiguity set based on probability trimmings. To make their model tractable, they resort to the widely known CVaR-based approximation of the JCC.

The aforementioned SAA method is another effective way to solve JCCPs and has the potential to identify OPF solutions with a better cost performance than that of the more conservative solutions delivered by the previous approaches. However, solving the JCC-OPF problem using SAA is challenging due to the presence of binary variables, the number of scenarios required and the size of the power systems. Lejeune & Dehghanian (2020) propose a methodology to solve the SAA of the JCC-OPF without including the power flow equations into the joint chance-constraint system. To the best of our knowledge, we are the first to efficiently solve the JCC-OPF problem by means of the SAA approach, using a MIP reformulation and including the arduous power flow constraints. Furthermore, unlike the sample-based approach introduced in Peña-Ordieres et al. (2021), which is based on a smooth nonlinear approximation of the JCC-OPF, ours offers optimality guarantees.

The performance of SAA is, nonetheless, directly contingent on the number of samples available. In particular, we refer the reader to the article by Luedtke & Ahmed (2008), where relations are established between the empirical acceptable probability of violation and the number of samples such that the SAA-based solution be feasible in the JCCP with a predefined confidence level. Statistical considerations apart, the main aim of this work is to prove that the proposed methodology leads to a substantial reduction of the computational burden of JCCPs addressed by a MIP SAA-based reformulation.

The main contribution of our work is the introduction of a new methodology to efficiently solve the SAA reformulation of the JCC-OPF. Our method solves the MIP to optimality, and is based on the combination of a tightening-and-screening procedure with the development of valid inequalities to obtain a formulation which is compact and tight at a time. We begin with a description of an iterative algorithm to strengthen the Big-Ms present in the mixed-integer reformulation of the JCC-OPF. Interestingly, although the procedure is not new (see Qiu et al. (2014)), we complement it with a screening procedure that allows us to eliminate an enormous percentage of the line and generator inequalities of the MIP. The screening procedure is possible due to the special features of our model, decisive to speed up the resolution of the instances proposed and, to the best of our knowledge, has not been applied to other CCPs before.

For ease of explanation and computation, the valid inequalities are proposed for the particular class of linear chance constraints present in the JCC-OPF, but our results are also applicable to more general types of CCPs, as we detail in Appendix B. We also show in Appendix A the relationship between our valid inequalities and the quantile cuts, stating that the addition of our inequalities yields a feasible region equivalent to the quantile closure of a specific relaxation of the MIP problem. The main advantage of our inequalities is that, unlike quantile cuts, they are not NP-hard to compute, and neither do they require a specific separation algorithm to include them dynamically (that is, they can all be included in the model from the outset). As many other techniques developed for JCCPs, our cuts also apply to the SCC-OPF. Finally, our valid inequalities extend the results introduced in

Roos & Widmayer (1994) for the *k-violation problem*, which can be seen as a mixed-integer linear problem (MILP) reformulation of a SCCP.

Finally, we test our resolution method through extensive computational results using standard power systems available in the related literature. The combination of the valid inequalities with the tightening of the Big-Ms and the screening procedure allows us to effectively solve to optimality instances that are not solved with the initial MIP formulation, since the combination of both techniques ostensibly reduces their size and difficulty. We also compare our resolution approach with state-of-the-art convex inner approximations of CCPs, in particular, the CVaR-based approximation, ALSO-X, and ALSO-X+ (Jiang & Xie (2022)).

The remainder of the paper is organized as follows. In Section 2 we introduce the main notation and the formulation of the JCC-OPF, the core problem of this work. Section 3 involves the reformulation of the problem into a MIP using the SAA approach and the proposed methodology: Subsection 3.1 describes the tightening and screening procedures, whereas Subsection 3.2 introduces the valid inequalities and the necessary algorithms to compute them. In Section 4 we present a case study, testing our results to solve instances of the DC OPF available in the literature. Section 5 points further research topics and includes some concluding remarks. Appendix A establishes the relationship between our valid inequalities and the quantile cuts present in the literature, and Appendix B discusses the generalization of our methodology and its possible application to other types of CCPs.

2. Optimal Power Flow under Uncertainty: A Joint Chance-Constrained Modeling Approach

In this section, we introduce the formulation of the OPF problem that we consider throughout this article. In its deterministic version, the OPF seeks to determine the least-costly dispatch of thermal generating units to satisfy the system *net* demand (i.e., demand minus renewable generation), while complying with the technical limits of production and transmission network equipment. However, given the inherently uncertain nature of the electricity net demand, the probabilistic version of the OPF problem can be formulated as a JCCP that aims at minimizing the expected production cost while enforcing that the technical constraints are satisfied with a given (high) probability.

The formulation of the JCC-OPF we present next is based on the following assumptions:

1. *Power system*: A power system consists of a set of buses (nodes), lines and generators which we denote by \mathcal{N} , \mathcal{L} and \mathcal{G} , in that order. We use indexes n , l and g to refer to elements in these sets, respectively. Furthermore, \mathcal{G}_n represents the set of generators connected to node n .
2. *Nodal net loads*: The (uncertain) electricity net demand at node n , \tilde{d}_n , is given by $\tilde{d}_n = d_n - \omega_n$, where d_n is the predicted value and ω_n is the forecast error with a change of sign. This error is modeled as a random variable with zero mean which follows an unknown continuous probability distribution.
3. *Generation*: To cope with the forecast errors $(\omega_n)_{n \in \mathcal{N}}$, generators' power outputs are adjusted according to the following affine control policy:

$$\tilde{p}_g = p_g - \beta_g \Omega, \quad \forall g \in \mathcal{G},$$

where $\Omega := \sum_{n \in \mathcal{N}} \omega_n$ is the system-wise aggregated forecast error, and p_g and β_g are the power output dispatch and the participation factor of generating unit g , respectively (see, e.g., Bienstock et al. (2014), Hou

& Roald (2020), Peña-Ordieres et al. (2021)). The minimum and maximum capacity of generator g is denoted by \underline{p}_g and \bar{p}_g , respectively.

4. *Power balance*: Given the affine control policy of the previous point, the power balance equation takes the following form:

$$\sum_{g \in \mathcal{G}} \tilde{p}_g - \sum_{n \in \mathcal{N}} \tilde{d}_n = \sum_{g \in \mathcal{G}} (p_g - \beta_g \Omega) - \sum_{n \in \mathcal{N}} (d_n - \omega_n) = 0.$$

Hence, to ensure the power balance for *any* realization of the forecast errors $(\omega_n)_{n \in \mathcal{N}}$, it must hold:

$$\begin{aligned} \sum_{g \in \mathcal{G}} p_g - \sum_{n \in \mathcal{N}} d_n &= 0 \\ \sum_{g \in \mathcal{G}} \beta_g &= 1. \end{aligned}$$

5. *Power flows*: Line flows are modeled using the well-known approximation based on the power transfer distribution factors (PTDFs), B_{ln} , $l \in \mathcal{L}$, $n \in \mathcal{N}$, which sets a linear relation between the power flow through line l and the power injected at node n . The maximum capacity of line l is denoted by \bar{f}_l .
6. *Power production cost*: The cost function of each generating unit is assumed to be quadratic and, as a result, the total power production cost is given by

$$\sum_{g \in \mathcal{G}} C_{2,g} (p_g - \Omega \beta_g)^2 + C_{1,g} (p_g - \Omega \beta_g) + C_{0,g},$$

where $C_{2,g}$, $C_{1,g}$, $C_{0,g}$ are the coefficients defining the quadratic cost function of generating unit g . On the assumption that ω_n , for each $n \in \mathcal{N}$, is a random variable with zero mean, we have (see, for instance, Peña-Ordieres et al. (2021))

$$\mathbb{E} \left[\sum_{g \in \mathcal{G}} C_{2,g} (p_g - \Omega \beta_g)^2 + C_{1,g} (p_g - \Omega \beta_g) + C_{0,g} \right] = \sum_{g \in \mathcal{G}} C_{2,g} p_g^2 + C_{1,g} p_g + C_{0,g} + \mathbb{V}(\Omega) C_{2,g} \beta_g^2,$$

where $\mathbb{V}(\Omega)$ denotes the variance of the random variable Ω .

With the above ingredients, the JCC-OPF problem that we tackle in this paper is formulated as follows:

$$\min_{p_g, \beta_g \geq 0, \forall g \in \mathcal{G}} \sum_{g \in \mathcal{G}} C_{2,g} p_g^2 + C_{1,g} p_g + C_{0,g} + \mathbb{V}(\Omega) C_{2,g} \beta_g^2 \quad (2a)$$

$$\text{s.t.} \quad \sum_{g \in \mathcal{G}} \beta_g = 1 \quad (2b)$$

$$\sum_{g \in \mathcal{G}} p_g - \sum_{n \in \mathcal{N}} d_n = 0 \quad (2c)$$

$$\underline{p}_g \leq p_g \leq \bar{p}_g, \quad \forall g \in \mathcal{G} \quad (2d)$$

$$-\bar{f}_l \leq \sum_{n \in \mathcal{N}} B_{ln} \left(\sum_{g \in \mathcal{G}_n} p_g - d_n \right) \leq \bar{f}_l, \quad \forall l \in \mathcal{L} \quad (2e)$$

$$\mathbb{P} \left(\begin{array}{l} \underline{p}_g \leq p_g - \Omega \beta_g \leq \bar{p}_g, \quad \forall g \in \mathcal{G} \\ -\bar{f}_l \leq \sum_{n \in \mathcal{N}} B_{ln} \left(\sum_{g \in \mathcal{G}_n} (p_g - \Omega \beta_g) + \omega_n - d_n \right) \leq \bar{f}_l, \quad \forall l \in \mathcal{L} \end{array} \right) \geq 1 - \epsilon. \quad (2f)$$

The objective (2a) is the minimization of the expected total generation cost. The equality constraints (2b) and (2c) enforce the power balance in the system, whereas constraints (2d) and (2e) ensure a feasible power dispatch which corresponds to an error-free scenario, i.e., to a realization of the net-load forecast errors such that $\omega_n = 0 \forall n \in \mathcal{N}$. Finally, expression (2f) constitutes the joint chance-constraint system by which the decision-maker states that the OPF solution must be feasible with a probability greater than or equal to $1 - \epsilon$. Accordingly, parameter ϵ is the maximum allowed probability of constraint violation set by the user. Formulation (2) is quite standard and has been used before by Bienstock et al. (2014), Hou & Roald (2020), Peña-Ordieres et al. (2021), among others.

Problem (2) can be written in the form of (1), i.e., as a CCP with linear JCC and random RHS and LHS. To see this, define the vector of continuous decision variables x in (1) as $x := (p_g, \beta_g)_{g \in \mathcal{G}}$, and group all these variables by means of the set \mathcal{I} with elements i running from 1 to $|\mathcal{I}| = 2|\mathcal{G}|$. In this way, we have that $x \in \mathbb{R}_+^{|\mathcal{I}|}$, the set $X \subseteq \mathbb{R}^{|\mathcal{I}|}$ represents the polyhedron defined by the deterministic constraints (2b)–(2e), and $f : \mathbb{R}^{|\mathcal{I}|} \rightarrow \mathbb{R}$ is the convex function providing the expected total generation cost (2a). Likewise, if we collect all the constraints involved in the joint chance-constraint system (2f) into the set \mathcal{J} (hence $|\mathcal{J}| = 2|\mathcal{G}| + 2|\mathcal{L}|$), this system can be represented by way of a technology matrix with random rows $a_j(\omega) \in \mathbb{R}^{|\mathcal{I}|}$, $j \in \mathcal{J}$, and random RHS $b_j(\omega) \in \mathbb{R}$, $j \in \mathcal{J}$, where the uncertainty is again represented through the random vector ω taking values in $\mathbb{R}^{|\mathcal{N}|}$.

The technology matrix in the joint chance-constraint system of the OPF problem (2) has a special structure. Indeed, each row $a_j(\omega)$ in this matrix can be rewritten as $a_j(\omega) = a_j^0 + \Omega(\omega)\hat{a}_j$, with $a_j^0, \hat{a}_j \in \mathbb{R}^{|\mathcal{I}|}$ and where $\Omega(\omega)$ is a real-valued function whose domain includes the support of ω . In our particular case, recall that $\Omega(\omega) = \sum_{n \in \mathcal{N}} \omega_n$. In Section 3.2, we exploit this special structure to dramatically facilitate the certification of the optimal OPF solution given our strategy to solve problem (2).

3. Solving the joint chance-constrained OPF via Sample Average Approximation

As discussed in the introduction, the CCP (2) can be easily reformulated into a MIP using SAA. Thus, we assume that ω has a finite discrete support defined by a collection of points $\{\omega_s \in \mathbb{R}^{|\mathcal{N}|}, s \in \mathcal{S}\}$ and respective probability masses $\mathbb{P}(\omega = \omega_s) = \frac{1}{|\mathcal{S}|}$, $\forall s \in \mathcal{S} = \{1, \dots, |\mathcal{S}|\}$. Accordingly, ω_{ns} and Ω_s are realizations of the respective random variables under scenario s . We define $p := \lceil \epsilon |\mathcal{S}| \rceil$, the vector y of binary variables y_s , $\forall s \in \mathcal{S}$, and the large enough constants $M_{gs}^1, M_{gs}^2, M_{ls}^3, M_{ls}^4$. Thus, the MIP reformulation of problem (2) writes as follows:

$$\min_{p_g, \beta_g \geq 0, y_s} \sum_{g \in \mathcal{G}} C_{2,g} p_g^2 + C_{1,g} p_g + C_{0,g} + \hat{\mathbb{V}}(\Omega) C_{2,g} \beta_g^2 \quad (3a)$$

$$\text{s.t.} \quad (2b) - (2e) \quad (3b)$$

$$p_g - \Omega_s \beta_g \geq \underline{p}_g - y_s M_{gs}^1, \quad \forall g \in \mathcal{G}, s \in \mathcal{S} \quad (3c)$$

$$p_g - \Omega_s \beta_g \leq \bar{p}_g + y_s M_{gs}^2, \quad \forall g \in \mathcal{G}, s \in \mathcal{S} \quad (3d)$$

$$\sum_{n \in \mathcal{N}} B_{ln} \left(\sum_{g \in \mathcal{G}_n} (p_g - \Omega_s \beta_g) - d_n + \omega_{ns} \right) \geq -\bar{f}_l - y_s M_{ls}^3, \quad \forall l \in \mathcal{L}, s \in \mathcal{S} \quad (3e)$$

$$\sum_{n \in \mathcal{N}} B_{ln} \left(\sum_{g \in \mathcal{G}_n} (p_g - \Omega_s \beta_g) - d_n + \omega_{ns} \right) \leq \bar{f}_l + y_s M_{ls}^4, \quad \forall l \in \mathcal{L}, s \in \mathcal{S} \quad (3f)$$

$$\sum_{s \in \mathcal{S}} y_s \leq p \quad (3g)$$

$$y_s \in \{0, 1\}, \quad \forall s \in \mathcal{S}. \quad (3h)$$

Constraints (3c)-(3f) represent the sample-based reformulation of the joint chance constraint (2f). For a given scenario $s \in \mathcal{S}$, inequalities (3c)-(3f) guarantee that all the original constraints are satisfied when $y_s = 0$. If $y_s = 1$, some of the original constraints can be violated for scenario s . Finally, the inequality (3g) ensures that the probability of the JCC is met and the binary character of variables y_s is declared in (3h). For simplicity and ease of notation, we reformulate model (3) as

$$\min_{x, y_s} f(x) \quad (4a)$$

$$\text{s.t. } x \in X \quad (4b)$$

$$\Omega_s \hat{a}_j^\top x - b_{js} + x^\top a_j^0 \leq M_{js} y_s, \quad \forall j \in \mathcal{J}, s \in \mathcal{S} \quad (4c)$$

$$\sum_{s \in \mathcal{S}} y_s \leq p \quad (4d)$$

$$y_s \in \{0, 1\}, \quad \forall s \in \mathcal{S}, \quad (4e)$$

where $x := (p_g, \beta_g)_{g \in \mathcal{G}}$, the deterministic feasible set X represents constraints (2b)-(2e), and constraint (4c) is a generalization of constraints (3c)-(3f). Note that we do not make any assumptions on the sign of \hat{a}_j^\top , b_{js} and a_j^0 . Using the generic formulation (4), we present in Subsection 3.1 a procedure to properly tune the values of the large constants M_{js} . We also explain in this subsection how the intermediate results of the tightening procedure can be efficiently used to remove constraints from set (4c) that are superfluous, thus making model (4) more compact. Finally, we introduce in Subsection 3.2 a set of valid inequalities that makes the linear relaxation of (4) remarkably tighter.

3.1. Tightening and Screening

It is well-known that the linear relaxation of a Big-M formulation tends to provide weak lower bounds in general (Conforti et al. (2014)). This is even more so when the Big-Ms are chosen too loose. Constants M_{js} in (4c) should be set large enough for the corresponding constraints to be redundant when the associated binary variables y_s are equal to 1, and *as small as possible* to tighten the MIP formulation. To this end, the literature provides an algorithm called “Iterative Coefficient Strengthening” (Qiu et al. (2014)). A customization of this procedure for the joint chance-constrained formulation (4) is detailed in Algorithm 1.

The output of Algorithm 1 is the tuned Big-Ms that are input to the MIP reformulation (4). This algorithm produces Big-Ms whose value either decreases or remains equal at each iteration. There is, in fact, a number of iterations beyond which the resulting Big-Ms converge. To reduce the computational burden of running Algorithm 1, all problems (5) in Step 2 can be solved in parallel. Hereinafter, we use the short name “ $\mathbf{T}(\kappa)$ ” (from “Tightening”) to refer to the solution of model (4) using the Big-M values given by the “Iterative Coefficient Strengthening” algorithm with κ iterations.

Equally important, Algorithm 1 can be easily upgraded to delete constraints (j, s) in (4c) that are redundant, and therefore, can be removed from problem (4). Indeed, if Algorithm 1 delivers a large constant $M_{js} \leq 0$, then constraint j in scenario s can be deleted from (4) without altering its feasible region or its optimal solution. This

Algorithm 1 Iterative Coefficient Strengthening

Input: The LHS and RHS coefficients $\{a_j^0, \hat{a}_j\}_{j \in \mathcal{J}}$ and $\{b_{js}\}_{j \in \mathcal{J}, s \in \mathcal{S}}$, respectively, the sample $\{\Omega_s\}_{s \in \mathcal{S}}$, and the maximum allowed violation probability p that determine the joint chance-constraint system (1c), the deterministic feasible set X , and the total number of iterations κ .

Output: The large constants $M_{js}, \forall j \in \mathcal{J}, s \in \mathcal{S}$.

Step 1. Initialization, $k = 0, M_{js}^0 = \infty, \forall j \in \mathcal{J}, s \in \mathcal{S}$.

Step 2. For each $j \in \mathcal{J}$ and $s \in \mathcal{S}$ update M_{js}^{k+1} as follows: If $M_{js}^k < 0$, then $M_{js}^{k+1} = M_{js}^k$. Otherwise,

$$M_{js}^{k+1} = \max_{x, y_s} x^\top a_j^0 + \Omega_s \hat{a}_j^\top x - b_{js} \quad (5a)$$

$$\text{s.t. } x \in X \quad (5b)$$

$$x^\top a_j^0 + \Omega_s \hat{a}_j^\top x - b_{js} \leq M_{js}^k y_s, \quad \forall j \in \mathcal{J}, s \in \mathcal{S} \quad (5c)$$

$$\sum_{s \in \mathcal{S}} y_s \leq p \quad (5d)$$

$$0 \leq y_s \leq 1, \quad \forall s \in \mathcal{S}. \quad (5e)$$

Step 3. If $k + 1 < \kappa$, then $k = k + 1$ and go to Step 2. Otherwise, stop.

is so because a non-positive M_{js} means that there is no x satisfying (5b)–(5e) such that the constraint takes on a value strictly greater than zero. Consequently, the constraint is redundant in (4), since the feasibility region of (5) is a relaxation of (4). This upgrade of method **T** not only makes formulation (4) tighter through coefficient strengthening, but also more compact by screening out redundant constraints. Naturally, the tightening and screening power of algorithm **T** increases at each iteration. From now on, we use the short name “**TS**(κ)” (from “Tightening and Screening”) to refer to the strategy whereby model (4) is solved without the constraints (4c) for which the value of M_{js} provided by Algorithm 1 after κ iterations is lower than or equal to 0.

While strengthening the parameters M_{js} is a common strategy in the technical literature to reduce the computational burden of CCPs, this is the first time, to our knowledge, that intermediate results of Algorithm 1 are used to eliminate superfluous constraints from model (4). We stress that the screening process itself comes at no cost from Algorithm 1, while removing superfluous constraints from (4) may substantially facilitate its solution. As we show in Section 4, this is particularly true for the JCC-OPF.

Apart from making formulation (4) more compact, the screening of superfluous constraints can also be used to accelerate the “Iterative Coefficient Strengthening” process at each iteration. To do so, it suffices to modify Algorithm 1 so that (5c) only includes the constraints for which $M_{js}^k > 0$. Thus, the number of constraints of model (5) is significantly reduced and so is its solution time.

3.2. Valid inequalities

In this section, we derive a set of valid inequalities to make the linear relaxation of problem (4) tighter. Furthermore, these valid inequalities can also be added to the constraint set (5) of Algorithm 1, thus dramatically increasing the tightening and screening power of **TS**. To facilitate the comparative analysis carried out in Section 4, the so upgraded algorithm is named “**TS+V**(κ)” (from “Tightening and Screening with Valid inequalities”).

To derive the set of valid inequalities for problem (4), we define the real variables $z_j \in \mathbb{R}$ as $z_j := \hat{a}_j^\top x$, and let

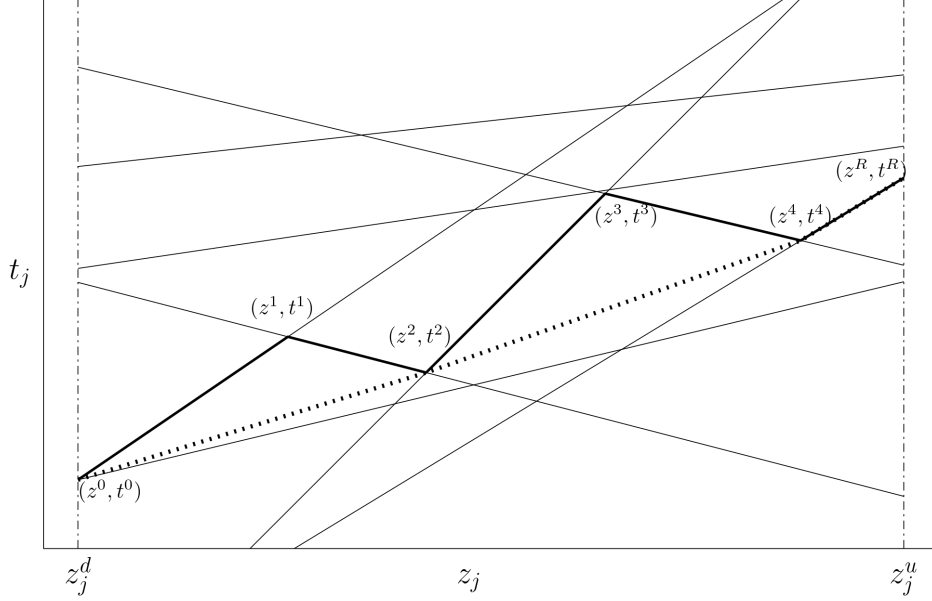


Figure 1: In bold, the 5-upper envelope (4-lower envelope, 4-level) of a set \mathcal{L}_j of 8 lines in the plane. In dotted, the lower hull of the 5-upper envelope

$z_j^d = \inf_{x \in X} \hat{a}_j^\top x$, $z_j^u = \sup_{x \in X} \hat{a}_j^\top x$ denote the lower and upper bounds on z induced by the polyhedral feasibility set (4b). Let us also define the function $L_{j_s} : f_{j_s}(z_j) = \Omega_s z_j - b_{j_s}$ for $z_j \in [z_j^d, z_j^u]$ and the set of functions $\mathcal{L}_j := \{L_{j_s}, \forall s \in \mathcal{S}\}$. The valid inequalities we propose are heavily supported by the concepts of k -lower and k -upper envelopes, which we define in the following.

Definition 3.1. For a given line L_{j_s} , we say that the point $(\tilde{z}, \tilde{t}) \in \mathbb{R}^2$ lies below, on or above function L_{j_s} depending on whether $\tilde{t} < \Omega_s \tilde{z} - b_{j_s}$, $\tilde{t} = \Omega_s \tilde{z} - b_{j_s}$ or $\tilde{t} > \Omega_s \tilde{z} - b_{j_s}$, respectively. Naturally, we also say that function L_{j_s} lies above, contains, or lies below point (\tilde{z}, \tilde{t}) in these cases. We also say that a point (\tilde{z}, \tilde{t}) belongs to the set of lines \mathcal{L}_j if there exists a line $L_{j_s} \in \mathcal{L}_j$ that contains the point (\tilde{z}, \tilde{t}) .

Definition 3.2. For a set of lines \mathcal{L}_j , the lower (resp. upper) score of a point is the number of lines in \mathcal{L}_j that lie below (resp. above) that point. The k -lower (resp. k -upper) envelope of a set of lines \mathcal{L}_j is the closure of the set of points that belong to \mathcal{L}_j and that have lower (resp. upper) score equal to $k - 1$. The k -lower envelope is also known as k -level.

For the sake of illustration, Figure 1 shows in bold the 5-upper envelope of a set of 8 lines. Clearly, the k -envelopes of sets \mathcal{L}_j can be seen as piece-wise linear functions on z_j .

Proposition 3.3. For a fixed $j \in \mathcal{J}$, let $U_j^{p+1}(\cdot)$ be the $(p+1)$ -upper envelope of the set of lines \mathcal{L}_j , with $p := \lfloor \epsilon |\mathcal{S}| \rfloor$. Then the inequality

$$U_j^{p+1}(\hat{a}_j^\top x) + x^\top a_j^0 \leq 0, \quad x \in X \quad (6)$$

is valid for problem (4).

Proof. Let \bar{x}, \bar{y} be any feasible solution of problem (4) with $\bar{z}_j = \hat{a}_j^\top \bar{x} \in [z_j^d, z_j^u]$, and suppose that $U_j^{p+1}(\bar{z}_j) + \bar{x}^\top a_j^0 > 0$. By definition of k -upper envelope, there exist $p+1$ lines in \mathcal{L}_j , $L_{j_{s_i}} : f_{j_{s_i}}(z_j) = \Omega_{s_i} z_j - b_{s_i} \forall i \in \{1, \dots, p+1\}$ such

that $f_{js_i}(\bar{z}_j) = \Omega_{s_i}\bar{z}_j - b_{s_i} \geq U_j^{p+1}(\bar{z}_j)$. Then for $i \in \{1, \dots, p+1\}$ it holds that $\Omega_{s_i}\bar{z}_j - b_{s_i} + \bar{x}^\top a_j^0 > 0$. Substituting in constraint (4c), we obtain that $\bar{y}_{s_i} M_{s_i} > 0 \Rightarrow \bar{y}_{s_i} = 1$, for $i \in \{1, \dots, p+1\}$. But then constraint (4d) is not satisfied, since $\sum_{s \in \mathcal{S}} \bar{y}_s \geq \sum_{i=1}^{p+1} \bar{y}_{s_i} = p+1 > p$. This is, however, in contradiction with our initial statement that \bar{x}, \bar{y} is a feasible solution of problem (4). \square

The technical literature already includes references that propose methodologies to determine the k -envelope of a set of linear functions. For instance, the authors of Cheema et al. (2014) give a basic algorithm for constructing k -envelopes called the Rider Algorithm. Essentially, this algorithm is based on the fact that the k -envelope is an unbounded polygonal chain that can be described by a sequence of vertices, which are intersections of lines of the set. In fact, every point in the k -envelope is contained in a given line. In this paper, we adapt the algorithm proposed in Cheema et al. (2014) to the particular case in which z_j^d, z_j^u are finite. Algorithm 2 describes our procedure in detail for a general set of the type \mathcal{L}_j .

Algorithm 2 Rider Algorithm to construct the k -upper envelope of \mathcal{L}_j (adapted to the bounded case)

To describe the k -upper envelope of a set of lines \mathcal{L}_j , we derive the sequence of vertices of the polygonal chain (intersections of lines in \mathcal{L}_j) $((z^0, t^0), \dots, (z^R, t^R))$ with $(z_j^d = z^0 < \dots < z^R = z_j^u)$.

- Step 1. Set $r = 0$. Let $\{(z_j^d, \Omega_s z_j^d - b_{js}), \forall s \in \mathcal{S}\}$, be the intersections of the lines $L_{js} \in \mathcal{L}_j$ with the vertical line $z = z_j^d$, and assume w.l.o.g. that all the points have different upper scores. Let $s_0 \in \mathcal{S}$ be such that the intersection $(z_j^d, \Omega_{s_0} z_j^d - b_{js_0})$ has upper score equal to $k+1$. Then $(z^0, t^0) = (z_j^d, \Omega_{s_0} z_j^d - b_{js_0})$.
 - Step 2. Compute the value of z_j for which the line L_{js_r} intersects the rest of the lines $L_{js} \in \mathcal{L}_j$ as $\text{int}_z(s, s_r) = \frac{b_{js} - b_{js_r}}{\Omega_s - \Omega_{s_r}}$.
If $\exists s' : z^r < \text{int}_z(s', s_r) < z^u$, go to Step 3. Otherwise, go to Step 4.
 - Step 3. Find the line that intersects L_{js_r} at the leftmost point to the right of z^r , that is, find $s_{r+1} = \arg \min_s \{\text{int}_z(s, s_r) : \text{int}_z(s, s_r) > z^r\}$. Set $(z^{r+1}, t^{r+1}) = (\text{int}_z(s_{r+1}, s_r), \Omega_{s_r} \text{int}_z(s_{r+1}, s_r) - b_{js_r})$, update $r = r+1$ and go to Step 2.
 - Step 4. Set $(z^R, t^R) = (z_j^u, \Omega_{s_r} z_j^u - b_{js_r})$.
-

The LHSs of the valid inequalities (6) are piece-wise linear functions not necessarily convex. Therefore, the inclusion of these inequalities into model (4) would require a significant amount of additional binary variables, which, in turn, is expected to increase the computational burden of this problem even further. Alternatively, we compute the lower hull of the k -upper envelope of \mathcal{L}_j , which takes the form of a convex piece-wise linear function. From this lower hull, we can extract a set of linear valid inequalities (the linear extensions of the pieces) that can be seamlessly inserted into model (4) without the need of any extra binary variables. In doing so, we are able to tighten model (4), which can thus be solved more efficiently by available optimization software. Before presenting the set of valid inequalities, the following definition is required.

Definition 3.4. *Let Z be the convex hull of a set of points P . The upper (resp. lower) hull of P is the set of edges of Z that lie on or above (resp. on or below) every point in P .*

Corollary 3.5 presents the set of linear valid inequalities (7) given by the lower hull of the k -upper envelope of \mathcal{L}_j .

Corollary 3.5. Let $\{(z^r, t^r)\}$, $r \in \{0, \dots, R\}$, be the ordered set of vertices obtained by applying Algorithm 2 to set \mathcal{L}_j , and let $\{(z^{r'}, t^{r'})\}$, $r' \in \{0, \dots, R'\} \subseteq \{0, \dots, R\}$, be the ordered subset of vertices such that the associated polygonal chain is the lower hull. Then the following linear inequalities

$$\frac{t^{r'+1} - t^{r'}}{z^{r'+1} - z^{r'}}(\hat{a}_j^\top x - z^{r'}) + t^{r'} \leq -x^\top a_j^0, \quad x \in X, r' \in \{0, \dots, R' - 1\} \quad (7)$$

are valid for problem (4).

Proof. The proof is straightforward, since for each $x \in X$ it holds $\frac{t^{r'+1} - t^{r'}}{z^{r'+1} - z^{r'}}(\hat{a}_j^\top x - z^{r'}) + t^{r'} \leq U_j^{p+1}(\hat{a}_j^\top x) \leq -x^\top a_j^0$, by hypothesis and using (6). \square

There exist plenty of algorithms of convexification of a set of points in the plane. Two of the most well-known are the *Jarvis march* and the *Graham scan* (Tóth et al. (2017)). Here, we give a simplified version of the former where we make use of special features of our set of points and only compute the lower hull. In particular, we assume that we have a set of presorted points $\{(z^r, t^r)\}$, $r \in \{0, \dots, R\}$ whose first and last points always belong to the hull. To speed up the process, we can find the point $(z^{\bar{r}}, t^{\bar{r}})$ from the previous set with the lowest t -coordinate (which always belongs to the lower hull), and then apply the algorithm to the subsets $\{(z^0, t^0), \dots, (z^{\bar{r}}, t^{\bar{r}})\}$ and $\{(z^{\bar{r}}, t^{\bar{r}}), \dots, (z^R, t^R)\}$. Algorithm 3 describes in detail the proposed convexification procedure.

Algorithm 3 Jarvis March Algorithm to obtain the lower hull of a set of presorted points P

Let $P = \{(z^r, t^r)\}$, $r \in \{0, \dots, R\}$ be a set of points with $z^0 < \dots < z^R$. The algorithm derives a subset $P' = \{(z^{r'}, t^{r'})\}$, $r' \in \{0, \dots, R'\} \subseteq \{0, \dots, R\}$, which constitutes the lower hull of the first set.

Step 1. Initially, set $P' = \{(z^0, t^0)\}$.

Step 2. Assume $(z^{r'}, t^{r'})$ is the last point included in P' . If $r' = R$, the lower hull of P is given by the set of points P' . Otherwise, let $r' + 1 := \arg \min_r \left\{ \frac{t^r - t^{r'}}{z^r - z^{r'}} : (z^r, t^r) \in P \text{ with } z^r > z^{r'} \right\}$. Update $P' = P' \cup \{(z^{r'+1}, t^{r'+1})\}$.

Repeat Step 2.

4. Numerical Experiments

This section discusses a series of numerical experiments with which we evaluate the different approaches presented in Section 3 to solve the SAA-based MIP reformulation of the JCC-OPF. In particular, we compare the performance of approaches **T**, **TS** and **TS+V** using five standard power systems widely employed in the technical literature on the topic, namely the IEEE-RTS-24, IEEE-57, IEEE-RTS-73, IEEE-118, and IEEE-300 test systems. All data pertaining to these systems are publicly available in the repository Power Grid Lib (2022) under version 21 and their main features are listed in Table 1. All optimization problems have been solved using GUROBI 9.1.2 (Gurobi Optimization, LLC (2022)) on a Linux-based server with CPUs clocking at 2.6 GHz, 6 threads and 32 GB of RAM. In all cases, the optimality GAP has been set to $10^{-9}\%$ and the time limit to 10 hours.

Similarly to Peña-Ordieres et al. (2021), we assume that the error of net loads is normally distributed, i.e., $\omega \sim N(\mathbf{0}, \Sigma)$, where $\mathbf{0}$ and Σ represent, respectively, the zero vector and the covariance matrix. We also assume that the standard deviation of ω_n at node n is proportional to the net nodal demand d_n according to a parameter ζ between 0 and 1. Thus, this parameter controls the magnitude of net demand fluctuations. Under these assumptions,

Table 1: Short Description of Test Power Systems

	IEEE-RTS-24	IEEE-57	IEEE-RTS-73	IEEE-118	IEEE-300
# Nodes	24	57	73	118	300
# Generators	32	4	96	19	57
# Lines	38	41	120	186	411

the procedure to model uncertainty proposed in Peña-Ordieres et al. (2021) runs as follows. First, we compute the positive definite matrix $C = \widehat{C}\widehat{C}^\top$ where each element of matrix \widehat{C} is a sample randomly drawn from a uniform distribution with support in $[-1, 1]$. Then, to obtain a positive definite matrix Σ in which the diagonal elements are equal to $(\zeta d_n)^2$, we define each of its entries ($\sigma_{nn'}$) as follows:

$$\sigma_{nn'} = \zeta^2 \frac{c_{nn'}}{\sqrt{c_{nn}c_{n'n'}}} d_n d_{n'}, \quad \forall n, n' \in \mathcal{N}.$$

where $c_{nn'}$ denotes the element of matrix C in row n and column n' . To avoid generating infeasible instances of the JCC-OPF problem, the parameter ζ has been set to 0.15 for the four smallest systems and to 0.05 for the IEEE-300 system. To characterize the net demand uncertainty, we consider 1000 scenarios and a tolerable probability of violation of the joint chance constraint of 5% (i.e., $\epsilon = 0.05$ and $p = 50$). Finally, each solution strategy is run for ten different sets of randomly generated samples. Accordingly, in this section we provide tables with figures averaged over these ten instances.

Table 2 includes the results of solving the mixed-integer quadratic optimization model (3) if the large constants M_{gs}^1 , M_{gs}^2 , M_{ls}^3 and M_{ls}^4 are set to a high enough arbitrary value, specifically 10^4 . Despite being remarkably computationally expensive, this approach has been used in the technical literature (e.g., Zhang et al. (2015)), and thus we refer to it as *benchmark approach* (**BN**). Table 2 includes the number of constraints in the model (**#CON**), the linear relaxation gap (**LR-GAP**) calculated using the optimal solution of each instance, the optimality gap given by the difference between the best lower bound and the best integer solution found by the MIP solver (**MIP-GAP**), the number of instances solved to global optimality in less than 10 hours (**#OPT**) and the solution time in seconds (**Time**). As expected, the computational time needed to solve the OPF with the Big-M model (3) increases significantly with the size of the instances. While the 10 instances from systems IEEE-RTS-24, IEEE-57 and IEEE-37 are solved in less than 10 hours, none of the instances for systems IEEE-118 and IEEE 300 are solved to global optimality within that time limit, and the average MIP-GAP after 10 hours amounts to 0.29% and 0.27%, respectively. Interestingly, despite the fact that the LR-GAP is relatively low for the IEEE-RTS-73 system, the average computational time required to solve this case is particularly high compared to the two smaller systems.

As discussed in the technical literature, a proper tuning of the Big-Ms makes model (3) tighter and generally easier to solve (Qiu et al. (2014)) by the MIP routine. Therefore, we evaluate the computational performance of the ‘‘Iterative Coefficient Strengthening’’ Algorithm and provide the corresponding results in Table 3. In particular, **T(1)**, **T(2)** and **T(3)** represent the results obtained by solving model (3) with the Big-M values provided by Algorithm 1 with $\kappa = 1, 2$ and 3 , respectively. Table 3 includes the average values of LR-GAP and MIP-GAP, the number of instances solved to optimality in less than 10 hours (**#OPT**) and the speedup factor with respect to the

Table 2: Benchmark approach (**BN**): Results

	IEEE-RTS-24	IEEE-57	IEEE-RTS-73	IEEE-118	IEEE-300
#CON	140143	168171	432435	410413	936939
LR-GAP	1.756%	0.623%	0.061%	0.956%	1.114%
MIP-GAP (#OPT)	0.00% (10)	0.00% (10)	0.00% (10)	0.29% (0)	0.27% (0)
Time (s)	1121.3	103.2	11161.2	36000.0	36000.0

benchmark approach. To determine this factor, we have considered that the total computational time of approach **T** is given as the sum of the time required to run Algorithm 1 κ times to determine the Big-Ms plus the time it takes to solve problem (3).

Table 3: Coefficient tightening approach (**T**): Results

		IEEE-RTS-24	IEEE-57	IEEE-RTS-73	IEEE-118	IEEE-300
LR-GAP	T (1)	1.755%	0.510%	0.061%	0.711%	0.472%
	T (2)	1.662%	0.330%	0.055%	0.522%	0.324%
	T (3)	1.386%	0.255%	0.029%	0.434%	0.264%
MIP-GAP (#OPT)	T (1)	0.00% (10)	0.00% (10)	0.00% (10)	0.27% (0)	0.16% (0)
	T (2)	0.00% (10)	0.00% (10)	0.03% (2)	0.16% (0)	0.09% (0)
	T (3)	0.00% (10)	0.00% (10)	0.00% (10)	0.12% (0)	0.07% (0)
Speedup factor	T (1)	0.22x	0.07x	0.61x	1.00x	1.00x
	T (2)	0.17x	0.13x	0.31x	1.00x	1.00x
	T (3)	0.48x	0.24x	0.66x	1.00x	1.00x

Since reducing the Big-M values makes model (3) tighter, the results in Table 3 show lower values of LR-GAP with respect to **BN**. Furthermore, this effect grows with the number of iterations since Algorithm 1 ensures that the Big-Ms never increase between iterations. Although decreasing the values of the Big-Ms leads to tighter MIPs for all the test systems, the numerical results in Table 3 clearly indicate that computational savings are not guaranteed in all cases. Indeed, while the ten instances are solved by **BN** in less than 10 hours for the IEEE-RTS-73 system, **T**(2) only provides the optimal solution for two instances. On top of that, the speedup factors for the three smaller systems are always lower than 1, which means that the computational times actually increase in these cases. On the contrary, the average MIP-GAP of the two largest systems is significantly decreased with respect to **BN**. Therefore, we conclude that, due to the heuristics implemented in current commercial MIP solvers, the computational advantages that one could expect a priori from “Iterative Coefficient Strengthening” are not always guaranteed and are contingent on the structure and data of the problem.

Next, in Table 4 we provide the computational results related to the **TS** method, in which Algorithm 1 is extended to remove redundant constraints from model (3). Here, #CON is provided as the percentage of the number of constraints of the reference model **BN** (indicated in Table 2) that are retained by **TS** in each iteration.

Table 4 also includes the average MIP-GAP, the number of instances solved to optimality and the average speedup factor in relation to **BN**.

Table 4: Tightening and Screening (**TS**): Results

		IEEE-RTS-24	IEEE-57	IEEE-RTS-73	IEEE-118	IEEE-300
#CON	TS(1)	23.9%	2.8%	26.0%	8.9%	12.7%
	TS(2)	23.3%	2.2%	23.8%	6.3%	9.1%
	TS(3)	23.1%	2.1%	23.0%	5.6%	8.0%
MIP-GAP (#OPT)	TS(1)	0.00% (10)	0.00% (10)	0.00% (10)	0.15% (0)	0.08% (0)
	TS(2)	0.00% (10)	0.00% (10)	0.00% (10)	0.03% (2)	0.04% (0)
	TS(3)	0.00% (10)	0.00% (10)	0.00% (10)	0.01% (6)	0.01% (4)
Speedup factor	TS(1)	1.5x	1.8x	4.7x	1.0x	1.0x
	TS(2)	1.5x	3.8x	2.6x	1.1x	1.0x
	TS(3)	3.8x	4.4x	15.1x	1.4x	1.2x

Table 4 shows that the upgraded Algorithm 1 screens out a huge percentage of the constraints in model (3), only retaining between 2% and 26% of them. The results in this table demonstrate that combining the tightening of the Big-Ms and the elimination of superfluous constraints leads to significant computational savings. For instance, the speedup factor for the three smallest systems ranges now between 1.5x and 15.1x. In addition, **TS(3)** is able to solve six and four instances to optimality for systems IEEE-118 and IEEE-300, respectively, in less than 10 hours, and the average MIP-GAP is reduced to 0.01% in these two largest power systems. Therefore, the computational performance of model (3) has been drastically improved by combining the strengthening of the Big-Ms (making model (3) tighter) and the removal of redundant constraints (making model (3) more compact). Equally important, the elimination of superfluous constraints largely reduces the need of the MIP solver for RAM memory, which decreases from around 100 GB in **T** to 32 GB in **TS**.

We continue the numerical experiments by evaluating the impact of including the valid inequalities derived in Section 3.2 into model (3). The so obtained results are collated in Table 5. In what follows, this approach is called **BN+V** for short. The results in Table 5 comprise, in order and following the previous notation, the average number of constraints, the average values of LR-GAP and MIP-GAP, the number of instances solved to optimality, and the average speedup factor with respect to the **BN** approach of Table 2.

Table 5: Tightening by valid inequalities (**BN+V**): Results

	IEEE-RTS-24	IEEE-57	IEEE-RTS-73	IEEE-118	IEEE-300
#CON	101.0%	101.2%	101.2%	101.6%	101.5%
LR-GAP	0.3374%	0.2038%	0.0001%	0.4784%	0.3192%
MIP-GAP (#OPT)	0.00% (10)	0.00% (10)	0.00% (10)	0.03% (1)	0.08% (0)
Speedup factor	46.4x	13.8x	65.2x	1.1x	1.0x

As can be seen, our valid inequalities only increase the total number of constraints by 1.0-1.6%. However, the LR-GAP is significantly reduced compared to that obtained by **BN**. This effect is particularly noticeable for the IEEE-RTS-73 system with an average value of the linear relaxation gap equal to 0.0001%, meaning that the linear relaxation of problem (3) with the proposed valid inequalities is very tight and its solution very close to the actual solution of that problem. Furthermore, the inclusion of the valid inequalities lead to average speedup factors that range between 13.8x and 65.2x for the three smallest systems. For the two largest systems, the time limit is reached in most instances, but the average MIP-GAP is reduced to 0.03% and 0.08%, respectively.

Finally, we present similar simulation results for the setup in which the valid inequalities are also used to boost the tightening and screening power of Algorithm 1 (that is, the valid inequalities are also included in problem (5)), leading to method **TS+V**. Table 6 provides the average number of constraints, the average values of LR-GAP and MIP-GAP, and the average speedup factor of **TS+V** with respect to **BN** in Table 2. Since increasing the number of iterations of Algorithm 1 barely affects the performance of **TS+V**, all the data shown in Table 6 correspond to $\kappa = 1$.

Table 6: Tightening and screening with valid inequalities (**TS+V**): Results

	IEEE-RTS-24	IEEE-57	IEEE-RTS-73	IEEE-118	IEEE-300
#CON	3.49%	1.61%	3.84%	2.68%	3.30%
LR-GAP	0.3365%	0.1519%	0.0001%	0.2821%	0.1603%
MIP-GAP (#OPT)	0.00% (10)	0.00% (10)	0.00% (10)	0.00% (10)	0.00% (10)
Speedup factor	706.8x	35.3x	1470.0x	23.1x	8.5x

The comparison of the results in Tables 4, 5 and 6 yields the following observations. First, including the valid inequalities in Algorithm 1 strengthens the Big-Ms even further, which in turn remarkably reduces the linear relaxation gap and increases the number of constraints identified as redundant in model (3). Indeed, the total number of constraints eventually retained by **TS+V** ranges between 1.61% and 3.84% if compared with **BN**. Second, **TS+V** can solve the 10 instances to global optimality in less than 10 hours for the five test systems considered in these numerical experiments. In fact, the optimal solutions obtained by **TS+V** are the ones we use to compute the values of the linear relaxation gap throughout these simulations. Third, **TS+V** is able to achieve speedup factors between 8.5x and 1470.0x depending on the test system. All in all, **TS+V** features the best computational performance in terms of resolution time and MIP-GAP among all the methods tested so far.

To conclude this study, in Table 7 the results of **TS+V** are contrasted with those provided by state-of-the-art approximations available in the literature. In particular, we consider the CVaR-based and ALSO-X conservative approximations, both described in Jiang & Xie (2022). Table 7 provides the average cost increase in percentage with respect to the optimal cost and the speedup factor with regard to **BN** for the different methodologies compared. As expected, the CVaR-based approximation leads to conservative results and involves average cost increases that range between 0.49% and 2.88%. Interestingly enough, **TS+V** computes the optimal solution and involves a higher speedup factor than the CVaR-based approach for two of the five systems. Compared with the two ALSO-X approximations, **TS+V** obtains the global optimal solution in all cases with speedup factors that are still

tantamount to those of these approximate methods.

Table 7: Comparison of the proposed **TS+V** approach and existing approximate methods

		IEEE-RTS-24	IEEE-57	IEEE-RTS-73	IEEE-118	IEEE-300
Average cost increase	TS+V	0.00%	0.00%	0.00%	0.00%	0.00%
	CVaR	2.88%	0.53%	1.71%	0.57%	0.49%
	ALSO-X	0.80%	0.08%	0.41%	0.08%	0.05%
	ALSO-X+	0.53%	0.07%	0.12%	0.05%	0.04%
Speedup factor	TS+V	706.8x	35.3x	1470.0x	23.1x	8.5x
	CVaR	387.1x	117.0x	265.1x	4045.5x	779.7x
	ALSO-X	18.0x	1.2x	21.3x	148.6x	11.13x
	ALSO-X+	7.8x	0.7x	6.6x	49.3x	3.7x

5. Conclusions and future research

In this paper, we propose a novel exact resolution technique for a MIP SAA-based reformulation of the JCC-OPF problem. Our methodology includes a screening method to eliminate superfluous constraints based on an iterative procedure to repeatedly tighten the Big-Ms present in the MIP. These procedures are combined with the addition of valid inequalities based on the special structure of the model. Said inequalities strengthen its linear relaxation and allow for additional screening of constraints. The resultant model is thus compact and tight.

In the case study, we show that, in comparison with the benchmark model, our methodology provides remarkable results in terms of the linear relaxation bounds, the RAM memory needed to solve the instances, and the total computational resolution time. Specifically, our method **TS+V** solves to optimality all of the instances generated for the IEEE-RTS-118 and the IEEE-RTS-300 test systems, the majority of which are not solved within 10 hours of computational time using the benchmark approach. Furthermore, the average number of constraints eliminated from all instances with **TS+V** always exceeds a 95% of them, and the lower bound is markedly increased by the inclusion of the valid inequalities, showing the outstanding results of the combination of the methods developed.

The comparison of our results with those provided by existing approximate methods shows that our approach is computationally very competitive for small and medium-sized instances, always providing the best results in terms of cost. For the large instances addressed, while outperformed by the approximate methods in terms of computational time (as expected), our exact solution strategy not only provides a certificate of optimality, but also returns the optimal solution within the set time limit. A promising future research line consists in the development of a generalized set of valid inequalities that combine variables from pairs or subgroups of lines and generators.

Acknowledgements

This work was supported in part by the European Research Council (ERC) under the EU Horizon 2020 research and innovation program (grant agreement No. 755705), in part by the Spanish Ministry of Science and Innovation

(AEI/10.13039/501100011033) through project PID2020-115460GB-I00, and in part by the Junta de Andalucía (JA) and the European Regional Development Fund (FEDER) through the research project P20_00153. Á. Porras is also financially supported by the Spanish Ministry of Science, Innovation and Universities through the University Teacher Training Program with fellowship number FPU19/03053. Finally, the authors thankfully acknowledge the computer resources, technical expertise, and assistance provided by the SCBI (Supercomputing and Bioinformatics) center of the University of Málaga.

Appendix A. Relationship with *quantile cuts*

Consider problem (1), with feasible region \mathcal{FR} , and let X be the set of deterministic constraints and $a_j(\omega) = a_j^0 + \Omega(\omega)\hat{a}_j$, $j \in \mathcal{J}$. For a given scenario $s \in \mathcal{S}$, define \mathcal{X}_s as the set of points that satisfy the constraints for that scenario, i.e.,

$$\mathcal{X}_s := \left\{ x \in \mathbb{R}^{|\mathcal{I}|} : \Omega_s \hat{a}_j^\top x \leq b_{js} - x^\top a_j^0, \quad \forall j \in \mathcal{J} \right\}.$$

To characterize the feasible region \mathcal{FR} , let $\mathcal{S}^F := \{S' \subseteq \mathcal{S} : |S'| \geq |\mathcal{S}| - p\}$ be the collection of all feasible subsets of scenarios. Then \mathcal{FR} can be represented as:

$$\mathcal{FR} := \bigcup_{S' \in \mathcal{S}^F} \left[X \bigcap_{s \in S'} \mathcal{X}_s \right].$$

In Xie & Ahmed (2018) it is proved that \mathcal{FR} can also be written in a conjunctive normal form. To do so, we introduce the definition of a *minimal partial covering subset*.

Definition A.1. *A set $S'' \subseteq \mathcal{S}$ is a partial covering subset if it intersects with all the feasible scenario subsets in \mathcal{S}^F , i.e., for any $S' \in \mathcal{S}^F$ we have $S' \cap S'' \neq \emptyset$. Also, a set S'' is a minimal partial covering subset if there does not exist another partial covering subset $\hat{S} \subseteq \mathcal{S}$ such that $\hat{S} \subsetneq S''$. Let \mathcal{S}^C denote the collection of all minimal partial covering subsets. When the samples are independent and identically distributed, like in our case, $\mathcal{S}^C := \{S'' \subseteq \mathcal{S} : |S''| = p + 1\}$.*

Proposition A.2 ((Xie & Ahmed 2018, Proposition 3)).

$$\mathcal{FR} = \bigcap_{S'' \in \mathcal{S}^C} \left[\bigcup_{s \in S''} (X \cap \mathcal{X}_s) \right].$$

Consider now the relaxation of problem (1) associated to a given row $j \in \mathcal{J}$:

$$\min_x f(x) \tag{A.1a}$$

$$\text{s.t. } \mathbb{P}\{a_j(\omega)^\top x \leq b_j(\omega)\} \geq 1 - \epsilon \tag{A.1b}$$

$$x \in X \tag{A.1c}$$

and its feasible region \mathcal{FR}_j . Clearly, it holds that $\mathcal{FR} \subseteq \bigcap_{j \in \mathcal{J}} \mathcal{FR}_j$. This is equivalent to considering the problem without joint constraints. In a similar manner, for a given scenario $s \in \mathcal{S}$ and row $j \in \mathcal{J}$, define \mathcal{X}_{js} as the set of points that satisfy the scenario for that row:

$$\mathcal{X}_{js} := \left\{ x \in \mathbb{R}^{|\mathcal{I}|} : \Omega_s \hat{a}_j^\top x \leq b_{js} - x^\top a_j^0 \right\},$$

with $\mathcal{X}_s = \cap_{j \in \mathcal{J}} \mathcal{X}_{js}$. Making use of the previous results, we have

$$\mathcal{FR}_j := \bigcup_{S' \in \mathcal{S}^F} \left[X \cap_{s \in S'} \mathcal{X}_{js} \right] = \bigcap_{S'' \in \mathcal{S}^C} \left[\bigcup_{s \in S''} (X \cap \mathcal{X}_{js}) \right].$$

Using this characterization of a relaxation of the feasible region, we are able to prove the following:

Proposition A.3. *Let $\mathcal{U}_j := \{x \in X : U_j^{p+1}(\hat{a}_j^\top x) \leq -x^\top a_j^0\}$. Then for $j \in \mathcal{J}$, $\mathcal{U}_j = \mathcal{FR}_j$.*

Proof. [$\mathcal{U}_j \subseteq \mathcal{FR}_j$] Assume $x \in \mathcal{U}_j$. Then $x \in X$ satisfies the chance constraint for (at least) $|\mathcal{S}| - p$ scenarios. But then, for any minimal partial covering $S'' \in \mathcal{S}^C$, since $|S''| = p + 1$, we must have $x \in \cup_{s \in S''} (X \cap \mathcal{X}_{js})$. Given that this occurs for any S'' , then x belongs to the intersection of S'' , and hence $x \in \mathcal{FR}_j$.

[$\mathcal{FR}_j \subseteq \mathcal{U}_j$] This proof is straightforward considering the validity of the proof of Proposition 3.3, but assuming $x \in \mathcal{FR}_j$ instead of $x \in \mathcal{FR}$. Thus, if $x \in \mathcal{FR}_j$, then x satisfies the single chance constraint j by definition. Since $\mathcal{U}_j^{p+1}(\hat{a}_j^\top x) \leq -x^\top a_j^0$ is a valid inequality for problem (A.1) associated to j , x must satisfy it as well. \square

Now, we are going to establish the relationship between our valid inequalities and the quantile closure described in Xie & Ahmed (2018). Let us first introduce the necessary definitions to relate the quantile closure with $\text{conv}(\mathcal{FR})$.

Definition A.4. *Given $\alpha \in \mathbb{R}^{|\mathcal{I}|}$, let $\{\gamma_s^\alpha(X)\}$ be the optimal values of*

$$\gamma_s^\alpha(X) := \min \{ \alpha^\top x : x \in X \cap \mathcal{X}_s \} \quad \forall s \in \mathcal{S}.$$

The $(1 - \epsilon)$ -quantile (or simply quantile) of $\{\gamma_s^\alpha(X)\}_{s \in \mathcal{S}}$ is denoted by $\gamma_q^\alpha(X)$ and is given by

$$\gamma_q^\alpha(X) := \min_{S' \in \mathcal{S}^F} \max_{s \in S'} \gamma_s^\alpha(X)$$

and the associated quantile cut is

$$\alpha^\top x \geq \gamma_q^\alpha(X).$$

Note that the definition of quantile cuts depends on X , a set of deterministic constraints that we may change if we apply cuts successively.

Definition A.5. *The first quantile closure of X is defined as*

$$X^1 := \bigcap_{\alpha \in \mathbb{R}^{|\mathcal{I}|}} \left\{ x \in \mathbb{R}^{|\mathcal{I}|} : \alpha^\top x \geq \gamma_q^\alpha(X) \right\}.$$

Inductively, we define the r th round quantile closure X^r as:

$$X^r := \bigcap_{\alpha \in \mathbb{R}^{|\mathcal{I}|}} \left\{ x \in \mathbb{R}^{|\mathcal{I}|} : \alpha^\top x \geq \gamma_q^\alpha(X^{r-1}) \right\} \quad r \geq 2.$$

Theorem A.6 ((Xie & Ahmed 2018, Theorem 1)).

$$X^1 = \bigcap_{S'' \in \mathcal{S}^C} \text{conv} \left[\bigcup_{s \in S''} (X \cap \mathcal{X}_s) \right], \tag{A.2}$$

and for each $r \geq 2$, $r \in \mathbb{Z}_{++}$,

$$X^r = \bigcap_{S'' \in \mathcal{S}^C} \text{conv} \left[\bigcup_{s \in S''} (X^{r-1} \cap \mathcal{X}_s) \right], \tag{A.3}$$

where $X^0 = X$.

Theorem A.7 ((Xie & Ahmed 2018, Theorem 2)). *The set sequence $\{X^r\}$ converges to $\text{conv}(\mathcal{FR})$ with respect to the Hausdorff distance; i.e., $\bar{X} := \lim_{r \rightarrow \infty} X^r = \text{conv}(\mathcal{FR})$.*

If, like previously, we consider these definitions applied to the relaxation of problem (1) that results from considering a single row $j \in \mathcal{J}$, then we can establish the following results:

Definition A.8. *Given $\alpha \in \mathbb{R}^{|\mathcal{I}|}$, let $\{\gamma_{js}^\alpha(X)\}$ be the optimal values of*

$$\gamma_{js}^\alpha(X) = \min \{ \alpha^\top x : x \in X \cap \mathcal{X}_{js} \} \quad \forall s \in \mathcal{S}.$$

The $(1 - \epsilon)$ -quantile (or simply quantile) of $\{\gamma_{js}^\alpha(X)\}_{s \in \mathcal{S}}$ is denoted by $\gamma_{jq}^\alpha(X)$ and is given by

$$\gamma_{jq}^\alpha(X) := \min_{S' \in \mathcal{S}^F} \max_{s \in S'} \gamma_{js}^\alpha(X),$$

and the associated quantile cut is

$$\alpha^\top x \geq \gamma_{jq}^\alpha(X).$$

Definition A.9. *The first quantile closure of X associated to $j \in \mathcal{J}$ is defined as*

$$X_j^1 := \bigcap_{\alpha \in \mathbb{R}^{|\mathcal{I}|}} \left\{ x \in \mathbb{R}^{|\mathcal{I}|} : \alpha^\top x \geq \gamma_{jq}^\alpha(X) \right\}.$$

Inductively, we define the r th round quantile closure X_j^r associated to $j \in \mathcal{J}$ as:

$$X_j^r := \bigcap_{\alpha \in \mathbb{R}^{|\mathcal{I}|}} \left\{ x \in \mathbb{R}^{|\mathcal{I}|} : \alpha^\top x \geq \gamma_{jq}^\alpha(X^{r-1}) \right\} \quad r \geq 2.$$

Theorem A.10 ((Xie & Ahmed 2018, Theorem 1)).

$$X_j^1 = \bigcap_{S'' \in \mathcal{S}^C} \text{conv} \left[\bigcup_{s \in S''} (X \cap \mathcal{X}_{js}) \right], \tag{A.4}$$

and for each $r \geq 2$, $r \in \mathbb{Z}_{++}$,

$$X_j^r = \bigcap_{S'' \in \mathcal{S}^C} \text{conv} \left[\bigcup_{s \in S''} (X_j^{r-1} \cap \mathcal{X}_{js}) \right], \tag{A.5}$$

where $X_j^0 = X$.

Theorem A.11 ((Xie & Ahmed 2018, Theorem 2)). *The set sequence $\{X_j^r\}$ converges to $\text{conv}(\mathcal{FR}_j)$ with respect to the Hausdorff distance; i.e., $\bar{X}_j := \lim_{r \rightarrow \infty} X_j^r = \text{conv}(\mathcal{FR}_j)$.*

Corollary A.12.

$$\mathcal{U}_j \subseteq \text{conv}(\mathcal{U}_j) = \bar{X}_j \tag{A.6}$$

This result is particularly relevant because, as is proven in the same work, the separation over the first quantile closure is, in general, NP-hard. Therefore, Corollary A.12 gives a way of deriving $\text{conv}(\mathcal{FR}_j)$ through the explicit set of valid inequalities (7).

Appendix B. Complexity and extension to the multidimensional case

Suppose there exist matrices $A_j \in \mathbb{R}^{q_j \times |\mathcal{I}|}$, $q_j \leq |\mathcal{I}|$ (this includes the identity), $j \in \mathcal{J}$, such that $a_j(\omega)$ in the chance constraint can be written as $a_j(\omega) = a_j^0 + \Omega(\omega)^\top A_j$, $j \in \mathcal{J}$, with $a_j^0 \in \mathbb{R}^{|\mathcal{I}|}$ and $\Omega(\omega)$ being a q_j -dimensional vector of real-valued functions whose domains include the support of ω . Note that the case described in Subsection 3.2 corresponds to $q_j = 1, \forall j \in \mathcal{J}$.

Now, define $z_j := A_j x$, with z_j^d and z_j^u being vectors containing the component-wise lower and upper bounds on z induced by the polyhedral feasibility set (4b). Then, we can define the sets of hyperplanes Π_j for $j \in \mathcal{J}$

$$\Pi_j := \{f_{js}(z_j) = \Omega_s^\top z_j - b_{js}, \quad \text{for } z_j \in B(z_j^d, z_j^u), \forall s \in \mathcal{S}\}, \quad (\text{B.1})$$

where $B(z_j^d, z_j^u) := \times_{i=1}^{q_j} [z_{ji}^d, z_{ji}^u]$.

The k -lower envelope in higher dimension is defined as follows:

Definition B.1. *Given a set of q -dimensional hyperplanes Π , the lower (resp. upper) score of a point t is the number of hyperplanes that lie strictly below (resp. strictly above) t . The k -lower (resp. k -upper) envelope is the closure of the set of points in Π that have lower (resp. upper) score equal to $k - 1$. The k -lower envelope is also known as the k -level.*

There is an extensive literature in the field of geometry dealing with the development of k -envelopes, since they find applications in seemingly unrelated problems like designing data structures (Chazelle & Preparata (1986), Clarkson (1987), Agarwal & Matoušek (1995)), processing ranking queries (Yu et al. (2012), Das et al. (2007), Shen et al. (2012), Cheema et al. (2014)) or solving hyperplane partitioning problems (Borobia (1994), Tóth (2000)). By geometric transformations, the time bounds found for k -envelopes also apply to closely related structures (and vice versa) like k -order Voronoi diagrams (Chan et al. (1997), Chazelle & Edelsbrunner (1987), Ramos (1999)), or k -belts and k -sets:

Definition B.2. *The k -belt of a set of hyperplanes Π , for $0 \leq k \leq \left\lceil \frac{|\Pi|}{2} \right\rceil$, is the closure of the set of points in the space that have lower and upper score greater than or equal to k .*

Definition B.3. *Given a fixed set T of points in \mathbb{R}^d , a k -set ($k \leq |T|$) of T is any subset of T of size k which can be separated from the complement of T by a hyperplane. The k -set problem seeks for the maximum possible number of k -sets.*

Figure B.2 shows (in light grey) the 4-belt of a set of 8 lines. Obviously, the boundary of the k -belt is the union of the k -upper and k -lower envelopes. Less obvious is the fact that k -envelopes and k -sets are closely related. In fact, using duality one can map a set of hyperplanes in \mathbb{R}^d (the primal space) into a set of points in \mathbb{R}^d (the dual space). For instance, in two dimensions it suffices to map a point (\tilde{z}, \tilde{t}) to a line $L : \tilde{z}z - \tilde{t}$ and vice versa. Hence, the worst-case complexity of the k -levels is within a constant factor of the worst-case number of k -sets in point sets (Dey (1998), Yu et al. (2012)).

In Edelsbrunner & Welzl (1986) it is proved that, if the intersections of lines are computed dynamically in their manner, then Algorithm 2 constructs the boundary of the k -belt of \mathcal{L} in $O(n \log^2 |\mathcal{L}|)$ time and $O(n + |\mathcal{L}|)$

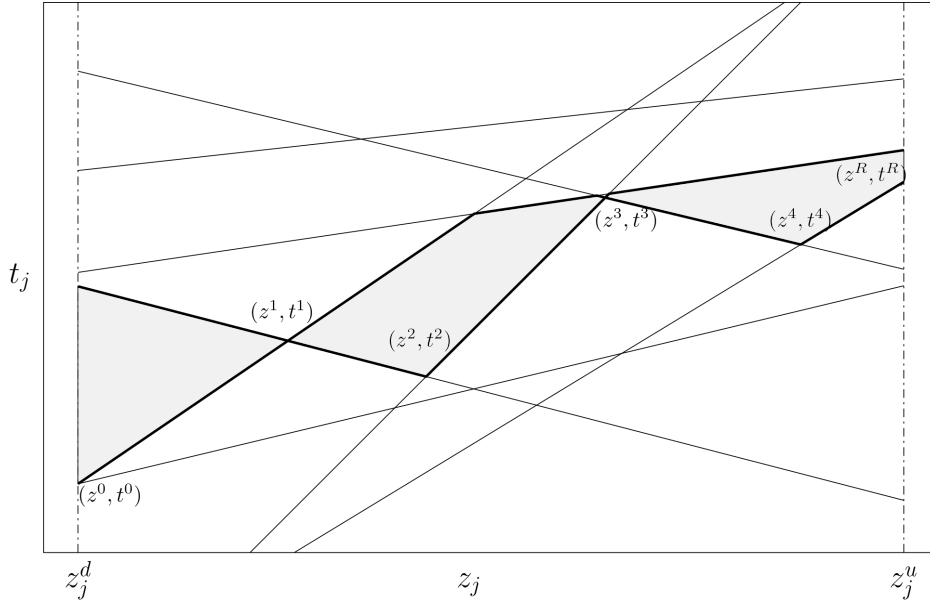


Figure B.2: In grey, the 4-belt of a set \mathcal{L}_j of 8 lines in the plane

space, where n denotes the maximum number of edges bounding the k -belt of any set \mathcal{L} . Dey (1998), Tóth (2000), Nivasch (2008) have subsequently improved the upper bound of the complexity on the k -set problem in the two-dimensional case. As for the development of efficient algorithms to compute k -envelopes or k -sets in higher dimensional spaces, they constitute a major challenge mainly because the computational complexity of k -envelopes increases exponentially with the increase in dimensionality (Agarwal & Matoušek (1995)). However, there exist algorithms for the cases $q = 3$ (Sharir et al. (2000), Ramos (1999), Tóth (2000)), $q = 4$ (Sharir (2011)) and $q \geq 5$ (Agarwal et al. (1998), Halperin & Sharir (2017)).

As for the convexification procedure, the convex hull problem is a classical problem with immense literature. The generalization of the Jarvis March to the multidimensional case is known as the *graph transversal method* (and also as the *gift-wrapping* algorithm), whereas the Graham Scan extension can be found under the name of *incremental method*. For small dimensions ($q = 2, 3$), we encounter parallel algorithms in the literature that use the *divide-and-conquer* paradigm to obtain better running times than the ones proposed here. However, we chose sequential ones for the ease of computation and explanation, and mainly because, given that the sets studied in our computational experiments are quite small, the difference in performance in the preprocessing steps is negligible. Surveys on algorithms and on the complexity of the convex hull problem can be found, for instance, in Tóth et al. (2017), Preparata & Shamos (2012).

References

- Abdi, A., & Fukasawa, R. (2016). On the mixing set with a knapsack constraint. *Mathematical Programming*, 157, 191–217.
- Agarwal, P. K., Aronov, B., Chan, T. M., & Sharir, M. (1998). On levels in arrangements of lines, segments, planes, and triangles. *Discrete & Computational Geometry*, 19, 315–331.
- Agarwal, P. K., & Matoušek, J. (1995). Dynamic half-space range reporting and its applications. *Algorithmica*, 13, 325–345.

- Ahmed, S., Luedtke, J., Song, Y., & Xie, W. (2017). Nonanticipative duality, relaxations, and formulations for chance-constrained stochastic programs. *Mathematical Programming*, *162*, 51–81.
- Ahmed, S., & Xie, W. (2018). Relaxations and approximations of chance constraints under finite distributions. *Mathematical Programming*, *170*, 43–65.
- Baker, K., & Bernstein, A. (2019). Joint chance constraints in ac optimal power flow: Improving bounds through learning. *IEEE Transactions on Smart Grid*, *10*, 6376–6385. doi:10.1109/TSG.2019.2903767.
- Ben-Tal, A., & Nemirovski, A. (2000). Robust solutions of linear programming problems contaminated with uncertain data. *Mathematical programming*, *88*, 411–424.
- Bienstock, D., Chertkov, M., & Harnett, S. (2014). Chance-constrained optimal power flow: Risk-aware network control under uncertainty. *SIAM Review*, *56*, 461–495.
- Borobia, A. (1994). Mirror property for nonsingular mixed configurations of lines and points in \mathbb{R}^3 . *Discrete & Computational Geometry*, *11*, 311–320.
- Chan, T. M., Snoeyink, J., & Yap, C.-K. (1997). Primal dividing and dual pruning: Output-sensitive construction of four-dimensional polytopes and three-dimensional Voronoi diagrams. *Discrete & Computational Geometry*, *18*, 433–454.
- Chazelle, B., & Edelsbrunner, H. (1987). An improved algorithm for constructing kth-order Voronoi diagrams. *IEEE Transactions on Computers*, *100*, 1349–1354.
- Chazelle, B., & Preparata, F. P. (1986). Halfspace range search: An algorithmic application of k-sets. *Discrete & Computational Geometry*, *1*, 83–93.
- Cheema, M., Shen, Z., Lin, X., & Zhang, W. (2014). A unified framework for efficiently processing ranking related queries. doi:10.5441/002/EDBT.2014.39.
- Chen, G., Zhang, H., Hui, H., & Song, Y. (2021). Time-efficient joint chance-constrained optimal power flow with a learning-based robust approximation. *arXiv preprint arXiv:2112.09827*, .
- Clarkson, K. L. (1987). New applications of random sampling in computational geometry. *Discrete & Computational Geometry*, *2*, 195–222.
- Conforti, M., Cornuéjols, G., & Zambelli, G. (2014). *Integer Programming* volume 271. Springer.
- Daniélsson, J., Jørgensen, B. N., de Vries, C. G., & Yang, X. (2008). Optimal portfolio allocation under the probabilistic VaR constraint and incentives for financial innovation. *Annals of Finance*, *4*, 345–367.
- Das, G., Gunopulos, D., Koudas, N., & Sarkas, N. (2007). Ad-hoc top-k query answering for data streams. In *Proceedings of the 33rd International Conference on Very Large Data Bases* (pp. 183–194).
- Dentcheva, D., Prékopa, A., & Ruszczyński, A. (2000). Concavity and efficient points of discrete distributions in probabilistic programming. *Mathematical Programming*, *89*, 55–77.
- Dey, T. K. (1998). Improved bounds for planar k-sets and related problems. *Discrete & Computational Geometry*, *19*, 373–382.
- Edelsbrunner, H., & Welzl, E. (1986). Constructing belts in two-dimensional arrangements with applications. *SIAM Journal on Computing*, *15*. doi:10.1137/0215019.
- Elçi, Ö., Noyan, N., & Bülbül, K. (2018). Chance-constrained stochastic programming under variable reliability levels with an application to humanitarian relief network design. *Computers & Operations Research*, *96*, 91–107.
- Esteban-Pérez, A., & Morales, J. M. (2021). Distributionally robust optimal power flow with contextual information. *arXiv preprint arXiv:2109.07896*, .

- Frank, S., Steponavice, I., & Rebennack, S. (2012). Optimal power flow: A bibliographic survey I. *Energy Systems*, *3*, 221–258.
- Günlük, O., & Pochet, Y. (2001). Mixing mixed-integer inequalities. *Mathematical Programming*, *90*, 429–457.
- Gurobi Optimization, LLC (2022). Gurobi Optimizer Reference Manual. URL: <https://www.gurobi.com>.
- Halperin, D., & Sharir, M. (2017). Arrangements. In *Handbook of Discrete and Computational Geometry* (pp. 723–762). Chapman and Hall/CRC. doi:10.1201/9781315119601-28.
- Henrion, R. (2007). Structural properties of linear probabilistic constraints. *Optimization*, *56*, 425–440.
- Henrion, R., & Strugarek, C. (2011). Convexity of chance constraints with dependent random variables: The use of copulae. In *Stochastic Optimization Methods in Finance and Energy* (pp. 427–439). Springer.
- Hong, L. J., Yang, Y., & Zhang, L. (2011). Sequential convex approximations to joint chance constrained programs: A Monte Carlo approach. *Operations Research*, *59*, 617–630.
- Hou, A. M., & Roald, L. A. (2020). Chance constraint tuning for optimal power flow. In *2020 International Conference on Probabilistic Methods Applied to Power Systems (PMAPS)* (pp. 1–6). doi:10.1109/PMAPS47429.2020.9183552.
- Jia, M., Hug, G., & Shen, C. (2021). Iterative decomposition of joint chance constraints in OPF. *IEEE Transactions on Power Systems*, *36*, 4836–4839.
- Jiang, N., & Xie, W. (2022). ALSO-X and ALSO-X+: Better convex approximations for chance constrained programs. *Operations Research*, .
- Küçükyavuz, S., & Jiang, R. (2021). Chance-constrained optimization: A review of mixed-integer conic formulations and applications. *arXiv preprint arXiv:2101.08746*, . arXiv:2101.08746.
- Lagoa, C. M., Li, X., & Sznaier, M. (2005). Probabilistically constrained linear programs and risk-adjusted controller design. *SIAM Journal on Optimization*, *15*, 938–951.
- Lejeune, M. A., & Dehghanian, P. (2020). Optimal power flow models with probabilistic guarantees: A boolean approach. *IEEE Transactions on Power Systems*, *35*, 4932–4935.
- Luedtke, J., & Ahmed, S. (2008). A sample approximation approach for optimization with probabilistic constraints. *SIAM Journal on Optimization*, *19*, 674–699.
- Luedtke, J., Ahmed, S., & Nemhauser, G. L. (2010). An integer programming approach for linear programs with probabilistic constraints. *Mathematical programming*, *122*, 247–272.
- Miller, B. L., & Wagner, H. M. (1965). Chance constrained programming with joint constraints. *Operations Research*, *13*, 930–945.
- Nair, R., & Miller-Hooks, E. (2011). Fleet management for vehicle sharing operations. *Transportation Science*, *45*, 524–540.
- Najjarbashi, A., & Lim, G. J. (2020). A decomposition algorithm for the two-stage chance-constrained operating room scheduling problem. *IEEE Access*, *8*, 80160–80172.
- Natarajan, K., Pachamanova, D., & Sim, M. (2008). Incorporating asymmetric distributional information in robust value-at-risk optimization. *Management Science*, *54*, 573–585.
- Nemirovski, A., & Shapiro, A. (2006). Scenario approximations of chance constraints. *Probabilistic and randomized methods for design under uncertainty*, (pp. 3–47).
- Nemirovski, A., & Shapiro, A. (2007). Convex approximations of chance constrained programs. *SIAM Journal on Optimization*, *17*, 969–996.

- Nivasch, G. (2008). An improved, simple construction of many halving edges. *Contemporary Mathematics*, 453, 299–306.
- Peña-Ordieres, A., Luedtke, J. R., & Wächter, A. (2020). Solving chance-constrained problems via a smooth sample-based nonlinear approximation. *SIAM Journal on Optimization*, 30, 2221–2250. URL: <https://doi.org/10.1137/19M1261985>. doi:10.1137/19M1261985. arXiv:<https://doi.org/10.1137/19M1261985>.
- Peña-Ordieres, A., Molzahn, D. K., Roald, L. A., & Wächter, A. (2021). DC optimal power flow with joint chance constraints. *IEEE Transactions on Power Systems*, 36, 147–158. doi:10.1109/TPWRS.2020.3004023.
- Power Grid Lib (2022). GitHub repository, available at: (<https://github.com/power-grid-lib/pglib-opf>).
- Prékopa, A. (2003). Probabilistic programming. *Handbooks in Operations Research and Management Science*, 10, 267–351.
- Preparata, F. P., & Shamos, M. I. (2012). *Computational Geometry: An Introduction*. Springer Science & Business Media.
- Qiu, F., Ahmed, S., Dey, S. S., & Wolsey, L. A. (2014). Covering linear programming with violations. *INFORMS Journal on Computing*, 26, 531–546. doi:10.1287/ijoc.2013.0582.
- Ramos, E. A. (1999). On range reporting, ray shooting and k-level construction. In *Proceedings of the Fifteenth Annual Symposium on Computational Geometry* (pp. 390–399).
- Roald, L., & Andersson, G. (2018). Chance-constrained AC optimal power flow: Reformulations and efficient algorithms. *IEEE Transactions on Power Systems*, 33, 2906–2918. doi:10.1109/TPWRS.2017.2745410.
- Rockafellar, R. T., & Uryasev, S. (2000). Optimization of conditional value-at-risk. *The Journal of Risk*, 2, 21–41. doi:10.21314/JOR.2000.038.
- Roos, T., & Widmayer, P. (1994). K-Violation linear programming. *Information Processing Letters*, 52, 109–114. doi:10.1016/0020-0190(94)00134-0.
- Shapiro, A. (2003). Monte Carlo sampling methods. *Handbooks in operations research and management science*, 10, 353–425.
- Sharir, M. (2011). An improved bound for k-sets in four dimensions. *Combinatorics, Probability and Computing*, 20, 119–129.
- Sharir, M., Smorodinsky, S., & Tardos, G. (2000). An improved bound for k-sets in three dimensions. In *Proceedings of the Sixteenth Annual Symposium on Computational Geometry* (pp. 43–49).
- Shaw, K., Irfan, M., Shankar, R., & Yadav, S. S. (2016). Low carbon chance constrained supply chain network design problem: A Benders decomposition based approach. *Computers & Industrial Engineering*, 98, 483–497.
- Shen, Z., Cheema, M. A., & Lin, X. (2012). Loyalty-based selection: Retrieving objects that persistently satisfy criteria. In *Proceedings of the 21st ACM International Conference on Information and Knowledge Management* (pp. 2189–2193).
- Song, Y., Luedtke, J. R., & Küçükyavuz, S. (2014). Chance-constrained binary packing problems. *INFORMS Journal on Computing*, 26, 735–747.
- Sun, H., Xu, H., & Wang, Y. (2014). Asymptotic analysis of sample average approximation for stochastic optimization problems with joint chance constraints via conditional value at risk and difference of convex functions. *Journal of Optimization Theory and Applications*, 161, 257–284. doi:10.1007/s10957-012-0127-1.
- Taleizadeh, A. A., Niaki, S. T. A., & Makui, A. (2012). Multiproduct multiple-buyer single-vendor supply chain problem with stochastic demand, variable lead-time, and multi-chance constraint. *Expert Systems with Applications*, 39, 5338–5348.
- Tanner, M. W., Sattenspiel, L., & Ntaimo, L. (2008). Finding optimal vaccination strategies under parameter uncertainty using stochastic programming. *Mathematical Biosciences*, 215, 144–151. doi:10.1016/j.mbs.2008.07.006.
- Tayur, S. R., Thomas, R. R., & Natraj, N. R. (1995). An algebraic geometry algorithm for scheduling in presence of setups and correlated demands. *Mathematical Programming*, 69, 369–401.

- Tóth, C. D., O'Rourke, J., & Goodman, J. E. (2017). *Handbook of Discrete and Computational Geometry*. CRC press.
- Tóth, G. (2000). Point sets with many k-sets. In *Proceedings of the Sixteenth Annual Symposium on Computational Geometry* (pp. 37–42).
- Van Ackooij, W., Zorgati, R., Henrion, R., & Möller, A. (2011). Chance constrained programming and its applications to energy management. *Stochastic Optimization-Seeing the Optimal for the Uncertain*, (pp. 291–320).
- Vrakopoulou, M., Margellos, K., Lygeros, J., & Andersson, G. (2013). Probabilistic Guarantees for the N-1 Security of Systems with Wind Power Generation. In *Reliability and Risk Evaluation of Wind Integrated Power Systems* (pp. 59–73). Springer.
- Xie, W., & Ahmed, S. (2016). On the quantile cut closure of chance-constrained problems. In *International Conference on Integer Programming and Combinatorial Optimization* (pp. 398–409). Springer.
- Xie, W., & Ahmed, S. (2018). On quantile cuts and their closure for chance constrained optimization problems. *Mathematical Programming*, 172, 621–646.
- Yu, A., Agarwal, P. K., & Yang, J. (2012). Processing a large number of continuous preference top-k queries. In *Proceedings of the 2012 ACM SIGMOD International Conference on Management of Data* (pp. 397–408).
- Zhang, Y., Shen, S., & Mathieu, J. L. (2015). Data-driven optimization approaches for optimal power flow with uncertain reserves from load control. In *2015 American Control Conference (ACC)* (pp. 3013–3018). IEEE.